

This is the accepted manuscript made available via CHORUS. The article has been published as:

Magnetic field effect on static antiferromagnetic order and  
spin excitations in the underdoped iron arsenide  
superconductor  $\text{BaFe}_{1.92}\text{Ni}_{0.08}\text{As}_2$

Miaoyin Wang, Huiqian Luo, Meng Wang, Songxue Chi, Jose A. Rodriguez-Rivera, Deepak Singh, Sung Chang, Jeffrey W. Lynn, and Pengcheng Dai

Phys. Rev. B **83**, 094516 — Published 14 March 2011

DOI: [10.1103/PhysRevB.83.094516](https://doi.org/10.1103/PhysRevB.83.094516)

# Magnetic field effect on static antiferromagnetic order and spin excitations in the underdoped iron arsenide superconductor iron $\text{BaFe}_{1.92}\text{Ni}_{0.08}\text{As}_2$

Miaoyin Wang,<sup>1</sup> Huiqian Luo,<sup>2</sup> Meng Wang,<sup>2,1</sup> Songxue Chi,<sup>3,4</sup> Jose A. Rodriguez-Rivera,<sup>3,4</sup>

Deepak Singh,<sup>3,4</sup> Sung Chang,<sup>3</sup> Jeffrey W. Lynn,<sup>3</sup> and Pengcheng Dai<sup>1,5,2,\*</sup>

<sup>1</sup>*Department of Physics and Astronomy, The University of Tennessee, Knoxville, Tennessee 37996-1200, USA*

<sup>2</sup>*Beijing National Laboratory for Condensed Matter Physics and Institute of Physics, Chinese Academy of Sciences, P. O. Box 603, Beijing 100190, China*

<sup>3</sup>*NIST Center for Neutron Research, National Institute of Standards and Technology, Gaithersburg, MD 20899, USA*

<sup>4</sup>*Department of Materials Science and Engineering,*

*University of Maryland, College Park, Maryland 20899, USA*

<sup>5</sup>*Neutron Scattering Science Division, Oak Ridge National Laboratory, Oak Ridge, Tennessee 37831-6393, USA*

We use neutron scattering to study the magnetic field effect on the static antiferromagnetic (AF) order and low-energy spin excitations in the underdoped iron arsenide superconductor  $\text{BaFe}_{1.92}\text{Ni}_{0.08}\text{As}_2$ . At zero field, superconductivity that occurs below  $T_c = 17$  K coincides with the appearance of a neutron spin resonance and reduction in the static ordered moment. Upon application of a  $\sim 10$ -T magnetic field in the FeAs-plane, the intensity of the resonance is reduced, accompanied by decreasing  $T_c$  and enhanced static AF scattering. These results are similar to those for some copper oxide superconductors, and demonstrate that the static AF order is a competing phase to superconductivity in  $\text{BaFe}_{1.92}\text{Ni}_{0.08}\text{As}_2$ .

PACS numbers: 74.25.Ha, 74.70.-b, 78.70.Nx

## I. I. INTRODUCTION

The parent compounds of iron arsenide superconductors exhibit static antiferromagnetic (AF) order with a simple collinear spin structure as shown in Fig. 1(a)<sup>1-3</sup>. Since superconductivity in iron arsenides can arise from electron or hole doping of their AF parent compounds<sup>4,5</sup>, it is generally believed that magnetism plays an important role in the superconductivity of these materials<sup>6-10</sup>. In one class of electron-doped iron arsenide based superconductors,  $\text{BaFe}_{2-x}(\text{Co,Ni})_x\text{As}_2$ <sup>11,12</sup>, superconductivity and static AF order can coexist in the underdoped regime<sup>13-15</sup>. Subsequent neutron scattering experiments on these samples reveal that the occurrence of superconductivity is accompanied by a reduction in the static AF Bragg intensity and the appearance of a neutron spin resonance in the magnetic excitations spectra<sup>16-18</sup>. Theoretically, it has been argued that the coexisting static AF order and superconductivity is inconsistent with the conventional BCS theory, but compatible with electron pairing mediated by quasiparticle excitations between sign reversed  $s$ -wave hole-like pockets around the  $\Gamma$  point and the electron-like Fermi pockets around the  $M$  point (the so-called  $s^\pm$  pairing symmetry)<sup>19-24</sup>. In this pure itinerant picture, electrons that form the ordered moment also contribute to the superconducting condensation, and AF order and superconductivity thus coexist microscopically<sup>23,24</sup>. If the static AF order in  $\text{BaFe}_{2-x}(\text{Co,Ni})_x\text{As}_2$  also has local moment contributions<sup>25,26</sup>, the magnetically ordered phase can coexist much easier with superconductivity but the ordered moment should not be affected by superconductivity<sup>24</sup>.

One way to test the interplay between magnetism and superconductivity is to use magnetic field as a tuning parameter. If the static AF order in the underdoped  $\text{BaFe}_{2-x}(\text{Co,Ni})_x\text{As}_2$  indeed coexists and competes with superconductivity<sup>15-18</sup>, application of a magnetic field that suppresses superconductivity should also enhance the static AF order, much like that of the electron-doped copper oxide superconductors<sup>27,28</sup>. On the other hand, if the static AF order in  $\text{BaFe}_{2-x}(\text{Co,Ni})_x\text{As}_2$  is chemically phase separated from the superconducting parts of the sample, application of a magnetic field should reduce the AF ordered moment, as has been found in chemically phase separated  $\text{Ba}_{1-x}\text{K}_x\text{Fe}_2\text{As}_2$ <sup>29</sup>. Neutrons cannot directly probe the microscopic nature of the coexisting state between static AF order and superconductivity<sup>16-18</sup>, but neutron scattering experiments in a magnetic field will allow a direct comparison on the effect of a field for the superconductivity and static AF order. In previous neutron scattering experiments on optimally doped iron arsenide  $\text{BaFe}_{0.9}\text{Ni}_{0.1}\text{As}_2$ <sup>30</sup>, a  $c$ -axis aligned magnetic field up to 14.5-T has been found to suppress the intensity of the neutron spin resonance and shift it to a lower energy corresponding to the field-induced reduction in  $T_c$ . Although such a field also reduces the magnitude of the spin gap, it is not sufficient to induce static AF order<sup>30</sup>. As a consequence, it is not clear static AF order is a competing phase to superconductivity. In a separate neutron scattering on iron chalcogenide  $\text{FeTe}_{0.5}\text{Se}_{0.5}$  superconductor<sup>31</sup>, a 7-T magnetic field parallel to the  $a$ - $b$  plane was found to reduce the intensity of the resonance. Similar to the results on  $\text{BaFe}_{0.9}\text{Ni}_{0.1}\text{As}_2$ <sup>30</sup>, a 7-T field was also insufficient to induce the static AF order in the sample<sup>31</sup>.

In this article, we report neutron scattering studies on the static AF order and spin excitations of underdoped

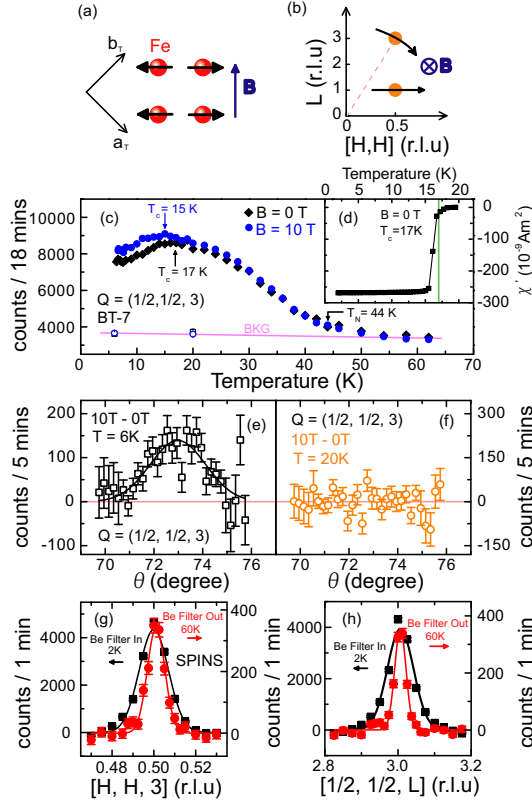


FIG. 1: (color online) (a) The antiferromagnetic spin structure of the undoped parent compound  $\text{BaFe}_2\text{As}_2$  and the direction of applied field. (b) The reciprocal space probed in the present experiment and the direction of applied field. (c) Temperature dependence of the AF Bragg peak at  $(0.5, 0.5, 3)$  at zero and 10-T in-plane field. The data were taken on BT-7 and showed  $T_N = 44$  K. The background scattering has no temperature and field dependence. (d) Temperature dependence of the Meissner and shielding signals on thin slabs of  $\text{BaFe}_{1.92}\text{Ni}_{0.08}\text{As}_2$ . These measurements were taken in zero field cooling (ZFC) with 5 Oe applied field along the thin slab's direction. (e) The field-on subtract field-off rocking curve scan through the  $(0.5, 0.5, 3)$  AF Bragg peak at 6 K. The positive scattering centered at the correct  $\theta$ -angle indicates that the field-induced effect occurs at the  $(0.5, 0.5, 3)$  AF Bragg position. (f) Identical rocking curve scans at 20 K, clearly indicating that the applied field has no observable effect on the static AF order below  $T_N$  and above  $T_c$ . (g) Black squares indicate a high-resolution scan along the  $[H, H, 3]$  direction in the AF ordered state. The red circles show the identical scan above  $T_N$  without the cold Be filter, which give  $\lambda/2$  scattering from the lattice structural Bragg peak  $(1, 1, 6)$ . (h) Similar scans along the  $[0.5, 0.5, L]$  direction.

$\text{BaFe}_{1.92}\text{Ni}_{0.08}\text{As}_2$  [ $T_c = 17$  K, Fig. 1(d)] under the influence of an applied magnetic field. At zero field, previous neutron scattering experiments on similar samples have shown that the static AF ordered moment reduces at the onset of superconductivity, together with the appearance of a neutron spin resonance in the magnetic excitation spectra<sup>16–18</sup>. We find that the static AF order in  $\text{BaFe}_{1.92}\text{Ni}_{0.08}\text{As}_2$  is not instrumental resolution limited, and has a spin-spin correlation length shorter than the lattice correlation length. Upon application of a magnetic field in the FeAs-plane, the static AF order is enhanced below  $T_c$ , but is not affected in the temperature range below  $T_N$  and above  $T_c$  ( $T_c < T < T_N$ ). The enhancement of the static AF order is accompanied by a suppression of the superconducting  $T_c$  and the intensity of neutron spin resonance. These results are consistent with a competing static AF order and superconductivity, and suggest that the interplay between magnetism and superconductivity in iron arsenide superconductors is similar in many ways to that for copper oxide superconductors.

## II. EXPERIMENTAL DETAILS

In recent inelastic neutron scattering experiments on underdoped  $\text{BaFe}_{1.906}\text{Co}_{0.094}\text{As}_2$  ( $T_c = 15$  K)<sup>16</sup>,  $\text{BaFe}_{1.92}\text{Co}_{0.08}\text{As}_2$  ( $T_c = 11$  K)<sup>17</sup>, and  $\text{BaFe}_{2-x}\text{Ni}_x\text{As}_2$ <sup>18</sup> superconductors, the static AF order was found to co-exist with superconductivity and cooling below  $T_c$ 's in these samples induced a weak neutron spin resonance in the magnetic excitations spectra at the expense of the AF Bragg peak intensity. For  $\text{BaFe}_{1.92}\text{Ni}_{0.08}\text{As}_2$  with  $T_c = 17$  K

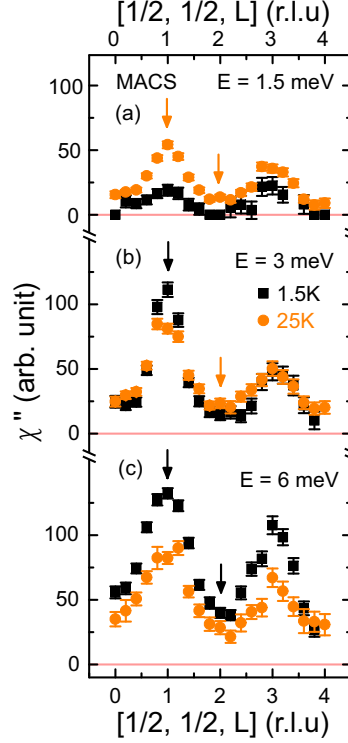


FIG. 2: (color online) Temperature dependence of the imaginary part of the dynamic susceptibility,  $\chi''(Q, \omega)$ , after subtracting the background scattering and correcting for Bose population factor. (a)  $Q$ -scans at  $E = 1.5$  meV along the  $[0.5, 0.5, L]$  direction above and below  $T_c$ . The data show clear  $L$ -direction sinusoidal modulation. (b) Similar scans at an energy just below the resonance ( $E = 3$  meV). (c)  $Q$ -scans at the resonance energy of  $E = 6$  meV. The intensity gain below  $T_c$  is clearly not uniform at different  $L$ -values.

[Fig. 1(d)], the static AF order occurs below  $T_N = 44$  K as shown in Fig. 1(c). To study the effect of an in-plane magnetic field on the static AF order and spin excitations, we have carried out neutron scattering experiments on the BT-7 thermal and SPINS cold triple-axis spectrometers<sup>18</sup> and on MACS cold neutron spectrometer<sup>32</sup> at the NIST Center for Neutron Research. We defined the wave vector  $Q$  at  $(q_x, q_y, q_z)$  as  $(H, K, L) = (q_x a / 2\pi, q_y b / 2\pi, q_z c / 2\pi)$  reciprocal lattice units (rlu) using the tetragonal nuclear unit cell, where  $a = 3.89$  Å,  $b = 3.89$  Å, and  $c = 12.77$  Å. We co-aligned about 5 grams of single crystal  $\text{BaFe}_{1.92}\text{Co}_{0.08}\text{As}_2$  in the  $[H, H, L]$  horizontal scattering plane (with mosaicity  $\sim 3^\circ$ ), and put our samples inside either a liquid He cryostat or a 12-T vertical field magnet. For thermal triple-axis measurements on BT-7, we used pyrolytic graphite (PG) as monochromator and analyzer with typical collimations of open-40'-S-40'-120' and the 15-T superconducting magnet system. The final neutron energy was chosen to be  $E_f = 13.5$  meV with a PG filter before the analyzer. For cold neutron SPINS and MACS measurements, we chose final neutron energy of  $E_f = 5.0$  meV with cold Be filters to eliminate  $\lambda/2$  scattering. Figure 1(a) shows the spin structure of the parent compound, and Figure 1(b) illustrates the reciprocal space probed in the experiments.

### III. RESULTS AND DISCUSSIONS

We first discuss our neutron scattering results on  $\text{BaFe}_{1.92}\text{Ni}_{0.08}\text{As}_2$  at zero field. The solid diamonds in Fig. 1(c) shows the temperature dependence of the magnetic scattering at  $Q = (0.5, 0.5, 3)$ . Consistent with earlier results on underdoped FeAs-based superconductors<sup>16–18</sup>,  $\text{BaFe}_{1.92}\text{Ni}_{0.08}\text{As}_2$  orders antiferromagnetically below a Néel temperature of  $T_N = 44$  K, and the magnetic Bragg intensity decreases below the onset of the superconducting  $T_c$ . To test if the AF order in  $\text{BaFe}_{1.92}\text{Ni}_{0.08}\text{As}_2$  is indeed long range and instrumental resolution limited, we carried out high resolution measurements on SPINS. First, we performed  $Q$ -scans along the  $[H, H, 3]$  and  $[0.5, 0.5, L]$  directions in the AF ordered state at 2 K with a cold Be filter before the analyzer to eliminate  $\lambda/2$  scattering [black squares in Figs. 1(g) and 1(h)]. We then carried out identical measurements in the paramagnetic state ( $T = 60$  K) without the Be filter before the analyzer using  $\lambda/2$  from the  $(1, 1, 6)$  nuclear Bragg peak as a probe of the instrumental resolution [red circles in Figs. 1(g) and 1(h)]. The outcome clearly suggests that the AF order in  $\text{BaFe}_{1.92}\text{Ni}_{0.08}\text{As}_2$  is not instrumental

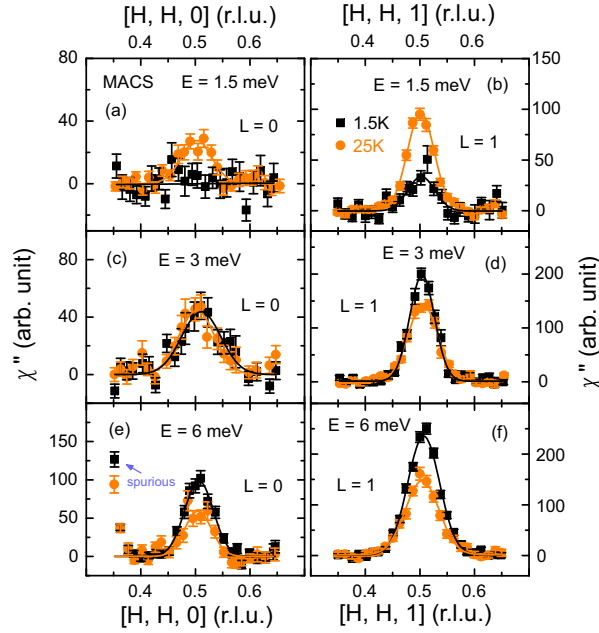


FIG. 3: (color online) Temperature dependence of  $\chi''(Q, \omega)$  along the  $[H, H, 0]$  and  $[H, H, 1]$  directions. (a) Constant-energy scans at  $E = 1.5$  meV along the  $[H, H, 0]$  direction across  $T_c$ . A clean spin gap is seen at this energy. (b) Identical scans along the  $[H, H, 1]$  direction, which show clear magnetic scattering centered at  $Q = (0.5, 0.5, 1)$  in the superconducting state. (c) Constant-energy scans at  $E = 3$  meV show no change in  $\chi''$  below and above  $T_c$  at  $Q = (0.5, 0.5, 0)$ . (d) The scattering clearly increases at  $Q = (0.5, 0.5, 1)$  below  $T_c$ . (e) Constant-energy scans at  $E = 6$  meV. The peak at  $Q = (0.7, 0.7, 0)$  is spurious. (f) Similar scans at  $E = 6$  meV across  $Q = (0.5, 0.5, 1)$ . Superconductivity clearly induces more magnetic scattering at  $Q = (0.5, 0.5, 1)$  than at  $Q = (0.5, 0.5, 0)$ .

resolution-limited. Solid lines in Fig. 1(g) and 1(h) are Gaussian fits to the peaks on linear backgrounds, where  $I = bkgd + I_0 \exp[-(H - H_0)^2/(2\sigma^2)]$  and the full-width-half-maximum  $\text{FWHM} = 2.3548\sigma$ . The in-plane measured peak and instrumental resolution FWHM's are 0.0165 and 0.0099 rlu, respectively. Along the  $c$ -axis, they are 0.0843 and 0.0363 rlu, respectively. To estimate the spin-spin coherence length ( $\xi$ ), we use Fourier transform of the Gaussian peaks. For the  $[H, H, L]$  scattering zone, the in-plane and  $c$ -axis spin-spin coherence lengths are  $\xi = [\sqrt{\ln(2)}/\pi](a/\sigma)$  and  $\xi = [\sqrt{2\ln(2)}/\pi](c/\sigma)$ , respectively<sup>27</sup>. By deconvoluting the instrumental effect, we estimate that the static AF spin-spin correlation lengths at  $T = 2$  K are  $\xi = 183 \pm 15$  Å in the FeAs-plane. Similarly, we find  $\xi = 148 \pm 10$  Å along the  $c$ -axis. For comparison, we note that the static AF order in  $\text{Ba}(\text{Fe}_{0.953}\text{Co}_{0.047})_2\text{As}_2$  with  $T_N = 47$  K and  $T_c = 17$  K<sup>16</sup> is long-range and instrument resolution-limited<sup>33</sup>.

To see if the static AF order in  $\text{BaFe}_{1.92}\text{Ni}_{0.08}\text{As}_2$  can be enhanced by application of a magnetic field, we carried detailed temperature dependent measurements at the AF Bragg peak position  $Q = (0.5, 0.5, 3)$  with and without a 10-T magnetic field applied along the  $[1, -1, 0]$  direction [Fig. 1(c)]. While a 10-T in-plane magnetic field has no observable effect on the Néel temperature and magnetic scattering above 20 K, it clearly enhances the magnetic scattering for temperatures below  $T_c$  compared to that of the zero field data. Figures 1(e) and 1(f) show the rocking curves of the field-on field-off difference plots at 5 K and 20 K, respectively. While a 10-T magnetic field has no influence on the static AF order at 20 K [Fig. 1(f)], it induces additional magnetic scattering at  $(0.5, 0.5, 3)$  below  $T_c$  [Fig. 1(e)].

In previous neutron scattering work on  $\text{BaFe}_{2-x}\text{Ni}_x\text{As}_2$ <sup>18,34–36</sup>, energy dispersive neutron spin resonances were found in the underdoped samples. However, it is not clear how spin excitations evolve and respond to superconductivity at energies below the resonance<sup>18</sup>. Figure 2 summarizes the effect of superconductivity on the  $c$ -axis modulations of the spin dynamic susceptibility  $\chi''(Q, \omega)$  at different energies obtained on MACS. At  $E = 1.5$  meV,  $\chi''(Q, \omega)$  displays a clear sinusoidal modulation along the  $L$ -direction centered at  $L = 1, 3, \dots$  in the normal state at  $T = 25$  K. Upon entering into the superconducting state ( $T = 1.5$  K), the scattering at  $L = 0, 2, 4, \dots$  vanishes indicating the presence of a spin gap while there are still magnetic scattering at  $L = 1, 3, \dots$ . These results are confirmed by constant-energy scans along the  $[H, H, L]$  direction with  $L = 0, 1$  [Figs. 3(a) and 3(b)], and are similar to the  $L$ -dependence of the spin gaps for the optimally electron-<sup>35,36</sup> and hole-doped<sup>37</sup> FeAs-based superconductors.

At an energy just below the resonance ( $E = 3$  meV),  $\chi''(Q)$  still has a strong  $L$ -modulation in both the normal and superconducting states [Fig. 2(b)]. On cooling from 25 K to 1.5 K,  $\chi''(Q)$  at  $Q = (0.5, 0.5, 1)$  enhances slightly but

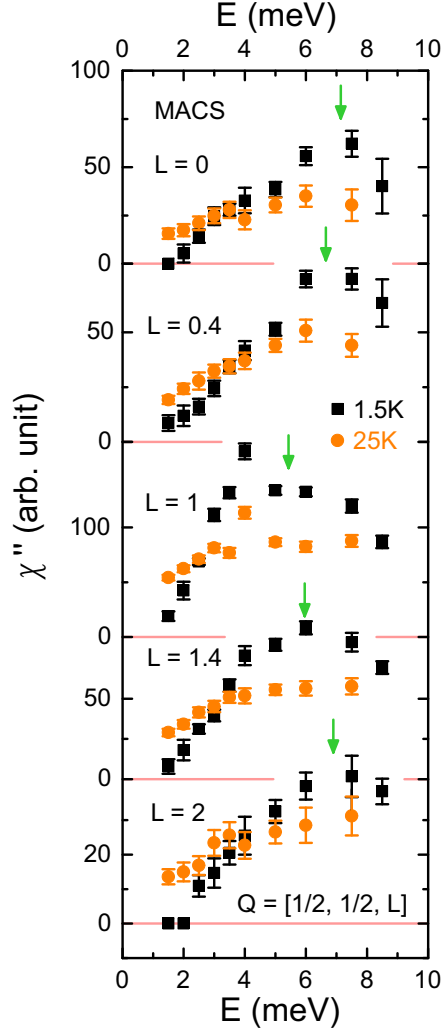


FIG. 4: (color online) Energy dependence of the dynamic susceptibility  $\chi''(\omega)$  above and below  $T_c$  for wave vectors  $Q = (0.5, 0.5, L)$  with  $L = 0, 0.4, 1, 1.4, 2$ . In the normal state,  $\chi''(\omega)$  increases with increasing energy at all  $L$  values. On entering into the superconducting state, the neutron spin resonance becomes dispersive and occurs at different energies for different  $L$ -values as marked by vertical arrows.

has no change at  $Q = (0.5, 0.5, 0)$ . Constant energy scans in Figs. 3(c) and 3(d) confirm these results. For an energy transfer near the resonance ( $E = 6$  meV), superconductivity enhances  $\chi''(Q)$  at all  $L$ -values as shown in Fig. 2(c). Constant-energy scans in Figs. 3(e) and 3(f) also show that the magnetic intensity gain at  $L = 0$  is smaller than that at  $L = 1$ . This is consistent with the dispersive nature of the resonance, where the mode shifts from  $\sim 7.5$  meV at  $L = 0, 2$  to  $\sim 5.8$  meV at  $L = 1$  shown in Fig. 4 similar to previous work on Co-doped  $\text{BaF}_{1.906}\text{Co}_{0.094}\text{As}_2$ <sup>38</sup>.

To determine if the enhanced static AF order in Fig. 1(c) under a magnetic field is compensated by a reduction in the intensity of the resonance and low-energy spin excitations, we carried out inelastic neutron scattering measurements under the influence of a magnetic field. Figure 5(a) shows constant- $Q$  scans carried out below and above  $T_c$  in zero and 11-T in-plane field at  $Q = (-0.5, -0.5, 1)$ . At zero field, the scan at 4.5 K shows a clear resonance peak near 6 meV. Upon application of a 11-T in-plane field, the intensity of the mode is reduced [Fig. 5(a)]. The zero and 11-T field difference plot at 4.5 K in Figure 5(b) shows a peak centered at 6 meV. Therefore, while a 14-T field applied along the  $c$ -axis can suppress the intensity and reduce the energy of the resonance, a 11-T field applied in the FeAs-plane only reduces the intensity of the resonance and does not affect the energy of the mode. This can be naturally explained by the vortex lattice effects in superconductors. A  $c$ -axis aligned magnetic field can suppress superconductivity much more efficiently than an in-plane field because the former induces supercurrent in the FeAs-plane, while vortex lattices in an in-plane field are present in-between the superconducting FeAs-planes. Figure 5(c) shows constant-energy scans in the superconducting state with and without the applied magnetic field. The effect of an applied field is to suppress

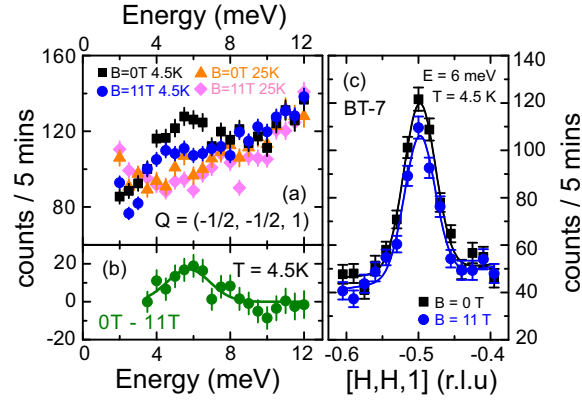


FIG. 5: (color online) Energy and wave vector dependence of the spin excitations as a function of an applied magnetic field in the FeAs-plane. (a) Constant- $Q$  scans at  $Q = (-0.5, -0.5, 1)$  below and above  $T_c$  at zero and 11-T in-plane field. Inspection of the raw data clearly reveals the reduction of the resonance intensity under field at  $T = 4.5$  K. (b) The field-off field-on difference plot at  $T = 4.5$  K shows that the magnetic scattering near the resonance energy is mostly affected by the applied field. (c) Constant-energy scans at the resonance energy for zero and 11-T field. The field-induced reduction in magnetic scattering occurs at the AF wave vector  $Q = (-0.5, -0.5, 1)$ .

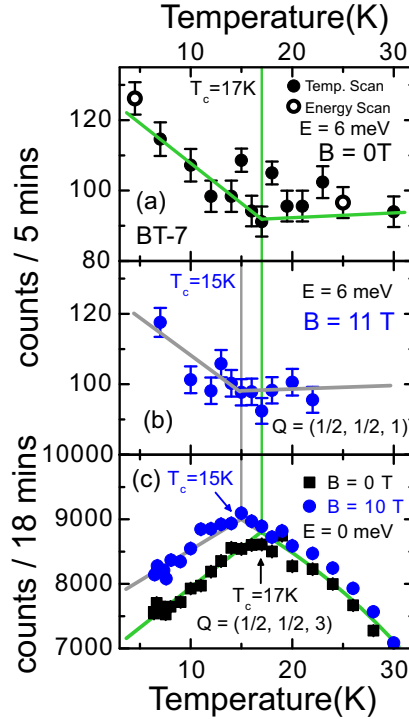


FIG. 6: (color online) Temperature dependence of the resonance and elastic scattering at zero field and 11-T in-plane field. (a) Temperature dependence of the  $E = 6$  meV scattering in zero field at  $Q = (0.5, 0.5, 1)$  for  $\text{BaFe}_{1.92}\text{Ni}_{0.08}\text{As}_2$ . The scattering increases in intensity below  $T_c$  of 17 K. (b) Identical temperature dependence of the  $E = 6$  meV scattering under 11-T field. The field-induced  $T_c$  has now shifted to 15 K. (c) Expanded plot of the elastic magnetic scattering in zero and 11-T field. The data confirm the shifted  $T_c$  under field.

magnetic scattering centered at the AF wave vector near the resonance energy.

Figure 6 shows the temperature dependence of the resonance at zero and 11-T. At zero field, the intensity of the mode increases gradually below  $T_c = 17$  K [Fig. 6(a)]. Under the influence of a 11-T field in the FeAs-plane, the resonance intensity starts to increase below about 15 K [Fig. 6(b)]. The reduced  $T_c$  in the in-plane field for the resonance is consistent with the reduction in the AF Bragg intensity as shown in Fig. 6(c). These results are also consistent with the expected  $T_c$  reduction from the transport measurements for similar  $T_c$  Co-doped materials<sup>39</sup>. If

we assume that the resonance is a direct probe for measuring electron pairing and superconductivity in iron arsenide superconductors, the observation of the elastic magnetic intensity gain at the expense of the resonance provides direct evidence that the static AF order in underdoped  $\text{BaFe}_{1.92}\text{Ni}_{0.08}\text{As}_2$  is competing with superconductivity.

We now discuss the implications of our results and compare them with that of the magnetic field effect in copper oxide superconductors. For the single layer hole-doped cuprate  $\text{La}_{2-x}\text{Sr}_x\text{CuO}_4$  near doping of  $x = 0.125$ , application of a magnetic field can enhance the static long-range AF order<sup>40–42</sup>. These results were initially interpreted as due to antiferromagnetism within the vortex cores of the superconductors under the field<sup>42</sup>, but has since been understood as due to proximity to the quantum critical point separating a purely superconducting phase from a superconducting/antiferromagnetism coexisting phase<sup>43,44</sup>. For the bilayer hole-doped cuprate  $\text{YBa}_2\text{Cu}_3\text{O}_{6+x}$ , while the initial neutron scattering experiments have shown that a field can suppress the intensity of the resonance<sup>45</sup>, the enhanced static order under a field has only recently been observed in underdoped  $\text{YBa}_2\text{Cu}_3\text{O}_{6.45}$ <sup>46</sup> and is not a universal phenomenon<sup>47</sup>. In the case of electron-doped cuprates, the enhanced static AF order under a field<sup>27</sup> is compensated by suppressing the intensity of the resonance<sup>28</sup>.

The observation of a field-induced enhancement of the static AF order at the expense of the resonance in underdoped iron arsenide superconductor  $\text{BaFe}_{1.92}\text{Ni}_{0.08}\text{As}_2$  is similar to the field-induced effects on the static AF order and resonance in some of the cuprate superconductors<sup>40–42,44,46</sup>, particularly the electron-doped materials<sup>27,28</sup>. Although our results indicate a competing static AF order with superconductivity, it is still unclear whether the static AF order in  $\text{BaFe}_{1.92}\text{Ni}_{0.08}\text{As}_2$  microscopically coexists with superconductivity as theoretically envisioned<sup>23,24</sup>. In recent muon spin rotation ( $\mu\text{SR}$ ) experiments on underdoped  $\text{BaFe}_{2-x}\text{Co}_x\text{As}_2$  with coexisting static AF and superconducting phases, the local magnetic field detected by muons does not show a noticeable reduction below  $T_c$ <sup>48</sup>. Since muons are local probes, this result suggests that the static AF moment of the system does not decrease below  $T_c$ . Therefore, the coexisting AF and superconducting phases might be mesoscopic, where superconductivity and AF order are intertwined in a very short length scale and live in separate regions. The relevant length parameter for superconducting regions is the superconducting coherence length, which is on the order of  $20 \text{ \AA}$ <sup>39</sup>. On the other hand, the propagation of the field from the static Fe moment to the muon site is due to dipolar interaction, which is much shorter than the penetration depth and dies away in about  $20 \text{ \AA}$ <sup>49</sup>. If the width of the superconducting rivers is smaller than the propagation range of the dipolar field, then the muons in the river regions can still feel the static internal field from the AF ordered background. In this scenario, application of a magnetic field that suppresses the superconducting parts of the sample enhances the static AF phase through volume fraction change (thus the reduction in the AF Bragg peak intensity) without changing the static ordered moment (no change in local field seen by  $\mu\text{SR}$ ). While this picture is consistent with the observation that the static AF order in  $\text{BaFe}_{1.92}\text{Ni}_{0.08}\text{As}_2$  is not resolution limited [Figs. 1(g) and 1(h)], it is inconsistent with the unchanged static spin-spin correlation lengths across  $T_c$  in  $\text{BaFe}_{1.92}\text{Co}_{0.08}\text{As}_2$ <sup>17</sup>. Furthermore, recent high-resolution soft X-ray resonant magnetic scattering results suggest that the static AF order in  $\text{BaFe}_{1.906}\text{Co}_{0.094}\text{As}_2$  is truly long-ranged<sup>33</sup>. Clearly, more systematic high-resolution neutron diffraction measurements are necessary to clarify the nature of the static AF ordered phase and its coexistence with superconductivity in  $\text{BaFe}_{2-x}(\text{Co},\text{Ni})_x\text{As}_2$ .

#### IV. IV. CONCLUSIONS

In summary, we have determined the effects of an in-plane magnetic field on the static AF order and spin excitations of the underdoped  $\text{BaFe}_{1.92}\text{Ni}_{0.08}\text{As}_2$  superconductor. At zero field, the system orders antiferromagnetically below about 44 K but the order is not truly long-ranged and instrumental resolution-limited. The spin excitations display sinusoidal modulation along the  $c$ -axis and form a dispersive neutron spin resonance associated with superconductivity as reported in earlier works<sup>18,34,36</sup>. While application of a magnetic field in the FeAs-plane has no observable effect on static AF order below  $T_N$  and above  $T_c$ , it clearly enhances the zero-field static AF order at the expense of the neutron spin resonance. Our results provide direct evidence that the static AF order is a competing phase to superconductivity. However, the present neutron scattering data cannot conclusively determine if the static AF order in  $\text{BaFe}_{1.92}\text{Ni}_{0.08}\text{As}_2$  is microscopically or mesoscopically coexisting with superconductivity.

#### V. V. ACKNOWLEDGEMENTS

We are grateful to Y. J. Uemura, G. M. Luke, and M. D. Lumsden for helpful discussions. The neutron scattering part of this work at UT/ORNL is supported by the U.S. NSF No. DMR-0756568, and by the U.S. DOE, Division of Scientific User Facilities. The single crystal growth and neutron scattering work at IOP is supported by Natural Science Foundation of China, the Ministry of Science and Technology of China (973 Project No. 2011CBA00110),



and Chinese Academy of Sciences.

- 
- \* Electronic address: [pdai@utk.edu](mailto:pdai@utk.edu)
- <sup>1</sup> C. de la Cruz, Q. Huang, J. W. Lynn, J. Li, W. Ratchliff II, J. L. Zarestky, H. A. Mook, G. F. Chen, J. L. Luo, N. L. Wang, Pengcheng Dai, *Nature (London)* **453**, 899 (2008).
  - <sup>2</sup> Jun Zhao, Q. Huang, C. de la Cruz, Shiliang Li, J. W. Lynn, Y. Chen, M. A. Green, G. F. Chen, G. Li, Z. Li, J. L. Luo, N. L. Wang, Pengcheng Dai, *Nature Materials* **7**, 953 (2008).
  - <sup>3</sup> Q. Huang, Y. Qiu, Wei Bao, J.W. Lynn, M.A. Green, Y. Chen, T. Wu, G. Wu, X.H. Chen, *Phys. Rev. Lett.* **101**, 257003 (2008).
  - <sup>4</sup> Y. Kamihara, T. Watanabe, M. Hirano, and H. Hosono, *J. Am. Chem. Soc.* **130**, 3296 (2008).
  - <sup>5</sup> M. Rotter, M. Tegel, and D. Johrendt, *Phys. Rev. Lett.* **101**, 107006 (2008).
  - <sup>6</sup> I. I. Mazin, D. J. Singh, M. D. Johannes, and M. H. Du, *Phys. Rev. Lett.* **101**, 057003 (2008).
  - <sup>7</sup> A. V. Chubukov, *Physica C* **469**, 640 (2009).
  - <sup>8</sup> F. Wang, H. Zhai, Y. Ran, A. Vishwanath, and D.-H. Lee, *Phys. Rev. Lett.* **102**, 047005 (2009).
  - <sup>9</sup> V. Cvetkovic and Z. Tesanovic, *Eur. Phys. Lett.* **85**, (2009).
  - <sup>10</sup> A. Moreo, M. Daghofer, J. A. Riera, and E. Dagotto, *Phys. Rev. B* **79**, 134502 (2009).
  - <sup>11</sup> A. S. Sefat, R. Jin, M. A. McGuire, B. C. Sales, D. J. Singh, and D. Mandrus, *Phys. Rev. Lett.* **101**, 117004 (2008).
  - <sup>12</sup> L. J. Li, Y. K. Luo, Q. B. Wang, H. Chen, Z. Ren, Q. Tao, Y. K. Li, X. Lin, M. He, Z. W. Zhu, G. H. Cao, and Z. A. Xu, *New J. Phys.* **11**, 025008 (2009).
  - <sup>13</sup> N. Ni, M. E. Tillman, J.-Q. Yan, A. Kracher, S. T. Hannahs, S. L. Budko, and P. C. Canfield, *Phys. Rev. B* **78**, 214515 (2008).
  - <sup>14</sup> J.-H. Chu, J. G. Analytis, C. Kucharczyk, and I. R. Fisher, *Phys. Rev. B* **79**, 014506 (2009).
  - <sup>15</sup> C. Lester, Jiun-Haw Chu, J. G. Analytis, S. C. Capelli, A. S. Erickson, C. L. Condon, M. F. Toney, I. R. Fisher, and S. M. Hayden, *Phys. Rev. B* **79**, 144523 (2009).
  - <sup>16</sup> D. K. Pratt, W. Tian, A. Kreyssig, J. L. Zarestky, S. Nandi, N. Ni, S. L. Budko, P. C. Canfield, A. I. Goldman, and R. J. McQueeney, *Phys. Rev. Lett.* **103**, 087001 (2009).
  - <sup>17</sup> A. D. Christianson, M. D. Lumsden, S. E. Nagler, G. J. MacDougall, M. A. McGuire, A. S. Sefat, R. Jin, B. C. Sales, and D. Mandrus, *Phys. Rev. Lett.* **103**, 087002 (2009).
  - <sup>18</sup> Miaoyin Wang, Huiqian Luo, Jun Zhao, Chenglin Zhang, Meng Wang, Karol Marty, Songxue Chi, Jeffrey W. Lynn, Astrid Schneidewind, Shiliang Li, and Pengcheng Dai, *Phys. Rev. B* **81**, 174524 (2010).
  - <sup>19</sup> I. I. Mazin and J. Schmalian, *Physica C* **469**, 614 (2009).
  - <sup>20</sup> T. A. Maier and D. J. Scalapino, *Phys. Rev. B* **78**, 020514(R) (2008).
  - <sup>21</sup> T. A. Maier, S. Graser, D. J. Scalapino, and P. Hirschfeld, *Phys. Rev. B* **79**, 134520 (2009).
  - <sup>22</sup> M. M. Korshunov and I. Eremin, *Phys. Rev. B* **78**, 140509(R) (2008).
  - <sup>23</sup> R. M. Fernandes, D. K. Pratt, W. Tian, J. Zarestky, A. Kreyssig, S. Nandi, M. G. Kim, A. Thaler, N. Ni, P. C. Canfield, R. J. McQueeney, J. Schmalian, and A. I. Goldman, *Phys. Rev. B* **81**, 140501(R) (2010).
  - <sup>24</sup> R. M. Fernandes and J. Schmalian, *Phys. Rev. B* **82**, 014521 (2010).
  - <sup>25</sup> C. Fang, H. Yao, W.-F. Tsai, J. P. Hu, and S. A. Kivelson, *Phys. Rev. B* **77**, 224509 (2008).
  - <sup>26</sup> C. Xu, M. Müller, and S. Sachdev, *Phys. Rev. B* **78**, 020501 (2008).
  - <sup>27</sup> H. J. Kang, P. Dai, H. A. Mook, D. N. Argyriou, V. Sikolenko, J. W. Lynn, Y. Kurita, S. Komiya, and Y. Ando, *Phys. Rev. B* **71**, 214512 (2005).
  - <sup>28</sup> S. D. Wilson, S. Li, J. Zhao, G. Mu, H.-h Wen, J. W. Lynn, P. G. Freeman, L.-P. Regnault, K. Habicht, Pengcheng Dai, *PNAS* **104**, 15259 (2007).
  - <sup>29</sup> J. T. Park, D. S. Inosov, Ch. Niedermayer, G. L. Sun, D. Haug, N. B. Christensen, R. Dinnebier, A.V. Boris, A. J. Drew, L. Schulz, T. Shapoval, U. Wolff, V. Neu, Xiaoping Yang, C. T. Lin, B. Keimer, and V. Hinkov, *Phys. Rev. Lett.* **102**, 117006 (2009).
  - <sup>30</sup> J. Zhao, L.-P. Regnault, C. L. Zhang, M. Y. Wang, Z. C. Li, F. Zhou, Z. X. Zhao, C. Fang, J. P. Hu, and P. C. Dai, *Phys. Rev. B* **81**, 180505(R) (2010).
  - <sup>31</sup> J. S. Wen, G. Y. Xu, Z. J. Xu, Z. W. Lin, Q. Li, Y. Chen, S. X. Chi, G. D. Gu, and J. M. Tranquada, *Phys. Rev. B* **81**, 100513 (2010).
  - <sup>32</sup> J. A. Ridriguez, D. M. Adler, P. C. Brand, C. Broholm, J. C. Cook, C. Brocker, R. Hammond, Z. Huang, P. Hundertmark, J. W. Lynn, N. C. Maliszewskyj, J. Moyer, J. Orndorff, D. Pierce, T. D. Pike, G. Scharfstein, S. A. Smee, and R. Vilaseca, *Meas. Sci. Technol.* **19**, 034023 (2008).
  - <sup>33</sup> M. G. Kim, A. Kreyssig, Y. B. Lee, J. W. Kim, D. K. Pratt, A. Thaler, S. L. Budko, P. C. Canfield, B. N. Harmon, R. J. McQueeney, and A. I. Goldman, *Phys. Rev. B* **82**, 180412(R) (2010).
  - <sup>34</sup> S. X. Chi, A. Schneidewind, J. Zhao, L. W. Harriger, L. J. Li, Y. K. Luo, G. H. Cao, Z. A. Xu, M. Loewenhaupt, J. P. Hu, and P. C. Dai, *Phys. Rev. Lett.* **102**, 107006 (2009).
  - <sup>35</sup> S. L. Li, Y. Chen, S. Chang, J. W. Lynn, L. J. Li, Y. K. Luo, G. H. Cao, Z. A. Xu, and P. C. Dai *Phys. Rev. B* **79**, 174527 (2009).
  - <sup>36</sup> J. T. Park, D. S. Inosov, A. Yaresko, S. Graser, D. L. Sun, Ph. Bourges, Y. Sidis, Y. Li, J.-H. Kim, D. Haug, A. Ivanov,

- K. Hradil, A. Schneidewind, P. Link, E. Faulhaber, I. Glavatsky, C. T. Lin, B. Keimer, and V. Hinkov, Phys. Rev. B **82**, 134503 (2010).
- <sup>37</sup> C. L. Zhang, M. Wang, H. Q. Luo, M. Y. Wang, M. S. Liu, J. Zhao, D. L. Abernathy, K. Marty, M. D. Lumsden, S. X. Chi, S. Chang, J. A. Rodriguez-Rivera, J. W. Lynn, T. Xiang, J. P. Hu, P. C. Dai, arXiv:1012.4065.
- <sup>38</sup> D. K. Pratt, A. Kreyssig, S. Nandi, N. Ni, A. Thaler, M. D. Lumsden, W. Tian, J. L. Zarestky, S. L. Budko, P. C. Canfield, A. I. Goldman, and R. J. McQueeney, Phys. Rev. B **81**, 140510 (2010).
- <sup>39</sup> A. Yamamoto, J. Jaroszynski, C. Tarantini, L. Balicas, J. Jiang, A. Gurevich, D. C. Larbalestier, R. Jin, A. S. Sefat, M. A. McGuire, B. C. Sales, D. K. Christen, and D. Mandrus, App. Phys. Lett. **94**, 062511 (2009).
- <sup>40</sup> S. Katano, M. Sato, K. Yamada, T. Suzuki, and T. Fukase, Phys. Rev. B **62**, 14677(R) (2000).
- <sup>41</sup> B. Khaykovich, Y. S. Lee, R. W. Erwin, S.-H. Lee, S. Wakimoto, K. J. Thomas, M. A. Kastner, and R. J. Birgeneau, Phys. Rev. B **66**, 014528 (2002).
- <sup>42</sup> B. Lake, H. M. Ronnow, N. B. Christensen, G. Aeppli, K. Lefman, D. F. McMorrow, P. Vorderwisch, P. Smeibidl, N. Mangkorntorn, T. Sasagawa, M. Nohara, H. Takagi, and T. E. Mason, Nature (London) **415**, 299 (2002).
- <sup>43</sup> Y. Zhang, E. Demler, and S. Sachdev, Phys. Rev. B **66**, 094501 (2002).
- <sup>44</sup> J. Chang, Ch. Niedermayer, R. Gilardi, N. B. Christensen, H. M. Ronnow, D. F. McMorrow, M. Ay, J. Stahn, O. Sobolev, A. Hiess, S. Pailhes, C. Baines, N. Momono, M. Oda, M. Ido, and J. Mesot, Phys. Rev. B **78**, 104525 (2008).
- <sup>45</sup> P. C. Dai, H. A. Mook, G. Aeppli, S. M. Hayden, and F. Doğan, Nature (London) **406**, 965 (2000).
- <sup>46</sup> D. Haug, V. Hinkov, A. Suchaneck, D. S. Inosov, N. B. Christensen, Ch. Niedermayer, P. Bourges, Y. Sidis, J. T. Park, A. Ivanov, C. T. Lin, J. Mesot, and B. Keimer, Phys. Rev. Lett. **103**, 017001 (2009).
- <sup>47</sup> C. Stock, W. J. L. Buyers, K. C. Rule, J.-H. Chung, R. Liang, D. Bonn, and W. N. Hardy, Phys. Rev. B **79**, 184514 (2009).
- <sup>48</sup> G. M. Luke and Y. J. Uemura, (private communications).
- <sup>49</sup> T. J. Williams, A. A. Aczel, E. Baggio-Saitovitch, S. L. Budko, P. C. Canfield, J. P. Carlo, T. Goko, H. Kageyama, A. Kitada, J. Munevar, N. Ni, S. R. Saha, K. Kirschenbaum, J. Paglione, D. R. Sanchez-Candela, Y. J. Uemura, and G. M. Luke, Phys. Rev. B **82**, 094512 (2010).